

CALORIMETER CONSIDERATIONS FOR A LINEAR COLLIDER DETECTOR

RAYMOND E. FREY

*Physics Department and Oregon Center for High Energy Physics
University Of Oregon
Eugene, OR 97403
E-mail: rayfrey@cosmic.uoregon.edu*

Current trends in the consideration of calorimeters for a future linear e^+e^- collider detector are discussed. The physics requirements and LC environment are briefly reviewed. The paradigm that excellent jet reconstruction can best be realized when the charged and neutral jet components are separated in the calorimeter is discussed. Design ideas are given, citing specific examples now under consideration in Europe, Asia, and N. America.

1. Introduction

A consensus has emerged internationally in the last two years that an e^+e^- linear collider (LC) in the energy range 0.5 to 1 TeV is the highest priority future project in elementary particle physics. Accelerator designs and test facilities in Europe, N. America, and Asia have made tremendous progress. This activity has inspired increased attention to LC detector design. Here, the prevalent ideas for calorimeter design are discussed. We start by highlighting the physics prospects, then discuss the LC detector environment, followed by design considerations and specific examples.

There is perhaps some feeling in the hadron collider community that e^+e^- detectors are straightforward, given the relatively benign LC environment, and perhaps do not merit significant R&D effort. However, I argue that this environment in fact allows one to think of detectors which are significantly better than the previous generation of excellent detectors at LEP and SLC. Hence, the LC provides an opportunity to achieve improved levels of physics measurement, and we should strive to take advantage of this. Calorimeters are perhaps undergoing the most extensive evolution in design to meet the LC challenge. An important element of the design philosophy is that the goal is not to build the best possible calorimeter, but rather the best possible *detector*. This highlights the fundamental interdependency of the calorimeter and other

sub-detectors in making a physics measurement. Our experience with previous detectors is pointing the way. But significant R&D will be required to take this next, significant step. And it is now underway.

2. Physics Requirements

In general, the main physics goals of the LC are the same as the LHC, namely to uncover the new physics responsible for electroweak symmetry breaking and to explore other phenomena at the TeV energy scale. Detectors must be prepared to study Higgs physics, supersymmetry (SUSY) if present, top physics, new and old gauge bosons, and so forth. While the LHC will likely be the discovery facility, the LC will be required to fully explore the physics. Perhaps one would expect scenarios similar to that of the W and Z bosons, where discovery at hadron colliders was followed by a full exploration of their properties at LEP/SLC. So the LC is expected to make measurements which are difficult or impossible at the LHC, but are essential for the elucidation of the underlying physics.

Perhaps the most important example, and the one most pertinent to calorimeter design, is the capability to measure electroweak processes which decay hadronically. In fact, multi-jet final states are common signatures of most new physics processes, many of which involve W and Z as intermediate states. Typical examples include the separation of the hadronic decays of WW from ZZ , or ZZ from ZH . Some important final states, such as HHZ to determine the Higgs self-coupling, have small cross sections and hence require the reconstruction of all final states, including those with 6 or more jets. Assuming that the detectors have this capability, the LC can provide these measurements.

In addition to jet final states, the LC physics also requires that leptons are well measured. Tau identification and measurement becomes very important at the LC, and is mentioned further below. SUSY final states require that the calorimeter coverage extend to small scattering angles, with no cracks.

There is no clear physics case at the LC for excellent photon energy resolution, such as that for $H \rightarrow \gamma\gamma$ at the LHC. On the other hand, some SUSY models predict secondary vertices where a photon is the only visible particle. Thus, one would like to identify photons which do not originate from the IP.

3. The LC Environment

The LC designs call for a maximum \sqrt{s} in the range 500 to 1000 GeV at a luminosity of a $2\text{--}4 \times 10^{34} \text{ cm}^{-2}\text{s}^{-1}$. The ease of low energy (M_Z) running is design dependent and a subject of current debate. A lovely feature of the LC is

that the collision IP is indeed a point. Along with the small beam radius, this allows excellent vertexing capability. The main environmental issues which drive calorimeter design are IP radiation and the accelerator bunch timing structure.

3.1. *The IP and IP Radiation*

The high charge density of the beams at the LC IP gives rise to photon radiation (beamstrahlung) and production of low energy e^+e^- pairs. Roughly 10^5 pairs are produced per beam crossing, as shown in Figure 1. Fortunately, the pairs have small, limited transverse momentum. Therefore, the detector solenoid prevents them from entering the detector proper. To allow the vertex detector to be ~ 1 cm from the IP, the field strength needs to be about 3 T or greater.

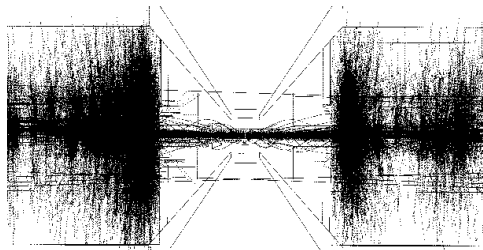


Figure 1. Pair production simulation from a LC bunch crossing. Note that the x and y scales are very different — the conical masks are about 2° from the beamline.

3.2. *Bunch Timing*

The TESLA and NLC/JLC designs have quite different timing structures. The differences are intrinsic to the linac RF technologies employed. For TESLA, bunch trains are supplied at 5 Hz. Each train has a length of 0.95 ms and the bunches cross every 337 ns. For NLC/JLC, the corresponding numbers are 150 Hz, 269 ns, and 1.4 ns. The physics event rate is small, but it is not yet clear if timing within a bunch train is required to avoid pile-up from 2-photon events and backgrounds. Individual bunch timing would clearly be a challenge at NLC, but should be readily achievable for the TESLA calorimeter.

One notes that there are lengthy intervals between bunch trains. This implies that power cycling of calorimeter electronics could provide large reductions of the heat load. The NLC (duty cycle 5×10^{-5}) provides an advantage in this case compared to TESLA (5×10^{-3}).

Finally, a small bunch crossing time interval requires a finite beam crossing angle to avoid additional unwanted bunch crossings. An angle of 20 (8) mrad is chosen for NLC (JLC). While a non-zero angle is not in principle necessary for TESLA, the zero-angle crossing design is technically difficult. A crossing angle has obvious implications for detectors placed at very small angle, but these detectors inside the masks are not discussed further here.

4. Making the Most of the Tracker: The Energy Flow Method

As discussed above, excellent jet reconstruction and measurement is the outstanding challenge for LC calorimeters. Two basic facts drive the approach to this measurement. First, jets are composed primarily of charged particles. For example, for $ZZ \rightarrow$ jets, the visible energy is 64% charged particles, 25% photons, and 11% neutral hadrons. (These numbers change very little for other hadronic final states.) Second, jet particles do not have large momenta, and the energy resolution for charged particles is vastly better in the tracker than the calorimeter. This last point is illustrated in Figure 2 which gives a typical momentum distribution, and in Figure 3 which compares tracker and calorimeter resolution for charged pions.

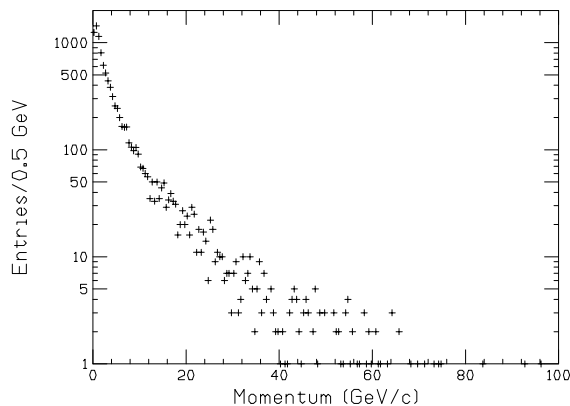


Figure 2. Typical charged particle momentum distribution for a multi-jet process, in this case $e^+e^- \rightarrow ZZ \rightarrow$ jets.

Clearly, one would like to take full advantage of the tracker for jet physics. In fact, this idea has been in use in e^+e^- detectors for ages, in one way or another. It is sometimes called “energy flow”, although there is no standard use of the term, as it is often used to describe the more far-reaching methodology

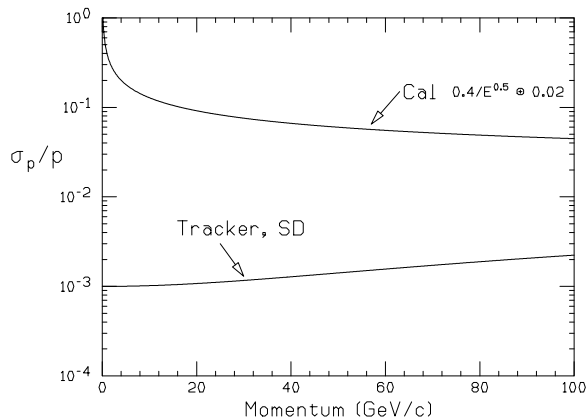


Figure 3. Comparison of typical single-particle energy resolution for charged pions for calorimetry and for an LC tracker. The tracker is the SD design with $\theta \approx 90^\circ$.

discussed below. In any case, at the LC we are in position to try to push the energy flow idea to a new level. Various approaches on how to achieve this are discussed in the next section. Finally, it is noted that energy flow will fail for sufficiently high \sqrt{s} due to higher track density and the eventual convergence of the single-particle resolution curves. Simulation studies indicate that this is well above 1 TeV.

4.1. Segmentation Requirement

Which strategy will best allow one to take advantage of the tracker measurement of the charged pions in jets? First, the photons will be measured in the electromagnetic calorimeter (ECal). So if one could make the ECal *transparent* to hadrons, then neglecting neutral hadrons, one would have excellent jet measurements — all the energy in the ECal would be from photons. This is illustrated in Figure 4(a). (Hence, it is helpful for the ratio of radiation length to interaction length, X_0/λ , to be relatively small for the ECal.) Unfortunately, a real ECal will have $\lambda \sim 1$, so our cartoon will often look like that in Figure 4(b). Without sufficient segmentation in the ECal, we cannot separate the photonic contribution(s) from that due to the pion(s). And in general, one would like to have segmentation in 3 dimensions to do this efficiently. Similarly, one needs to separate charged and neutral hadrons in the hadron calorimeter (HCal) in order to take advantage of this method.

The highly segmented approach to the implementation of energy flow is the one adopted by the TESLA and the American SD designs, discussed below.

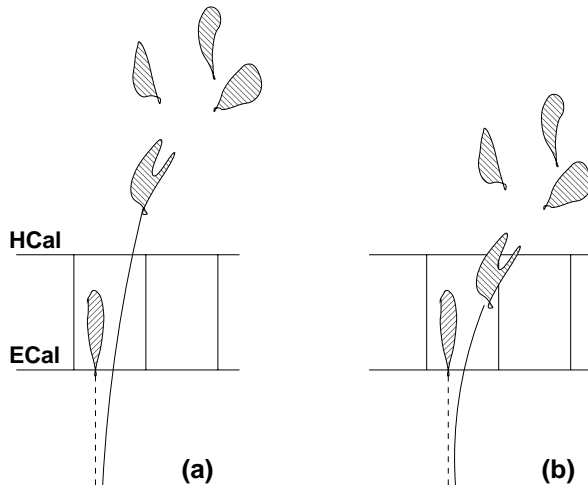


Figure 4. Illustration of the interaction of a π^0 and a π^+ from a jet in a cartoon calorimeter. The π^+ does not interact in the ECal in (a), but does in (b). The ECal has no longitudinal segmentation and the transverse segmentation is indicated.

Two other approaches can be considered. One might emphasize the ECal energy resolution by using crystals. Here, one has the problem with lack of segmentation illustrated in Figure 4, but would presumably try to correct using average energy depositions. CMS has shown that this is helpful.¹ One would presumably include small X_0/λ as a design criterion.

Finally, one can emphasize the hadronic response of the calorimeter by choosing one which provides hardware compensation. Charged/neutral separation would still be necessary, and it is difficult to find a technology which combines compensation with excellent segmentation. This is the approach of the JLC and American LD detector designs.

4.2. Requirements for the Electromagnetic Calorimeter

In considering ECal segmentation, one should first examine what is implied from LC jet physics and the detector induced charged particle sagitta, which is proportional to BR^2 . A typical example is given in Figure 5 for the SD detector. We see that the physics requires a separation at the level of ≈ 1 cm. Hence, we strive to use a small Molière radius, tungsten being an obvious choice with $R_m = 0.9$ cm. A figure of merit is BR^2/R_m . Finally, the segmentation need to be comparable to R_m , smaller if possible. The TESLA and SD designs implement this segmentation using silicon detectors throughout the ECal, amounting to $\sim 10^3$ m² of silicon.

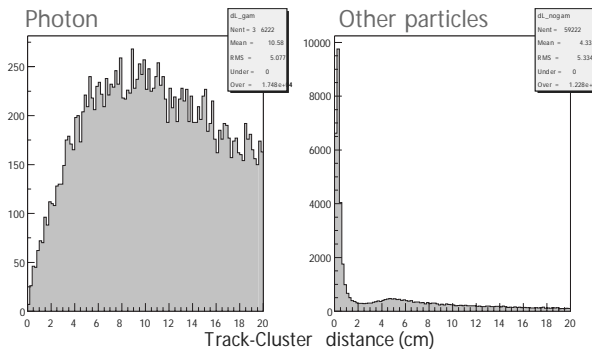


Figure 5. Example of ECal transverse segmentation requirement for $e^+e^- \rightarrow t\bar{t} \rightarrow$ jets for the SD detector. The left-hand figure gives the transverse separation between the charged particle position determined in the ECal and the centroid of all photon showers. The right-hand figure is the transverse separation between charged particles as determined by the ECal and the tracker. Figure from M. Iwasaki.

A dense, highly segmented ECal provides other important assets. It allows tracking of MIPs to extend into the calorimeter. As we point out below, this is important for the HCal, too. It also provides photon tracking, which opens the possibility to find photons not originating from the IP, potentially a critical signature for new physics. Figure 6 shows a display from a GEANT4 study of photon tracking in the SD detector. The resolution on the extrapolation to the IP was found to be 3.5 cm in both r - ϕ and z for 10 GeV photons. The same study applied to charged particles found a 1 cm error.

Numerous physics studies have pointed out the importance of identifying τ 's. Also, because of the benefits of using the tau as a polarimeter, one might demand that the calorimeter have the ability to identify some specific decay modes. Figure 7 shows that with sufficient granularity, one of these decay modes can be identified even at very high boost.

4.3. Requirements for the Hadronic Calorimeter

While hadronic showers are large and diffuse, one still expects a highly segmented HCal to be very important, primarily because tracking MIPs through the HCal is seen to be a key element in energy flow pattern recognition. Here is an outline of how this information might be used: One would do tracking of charged particles in the HCal. If they do not interact, they are probably muons (to be verified with a muon detection system). If a track terminates at a shower(s), begin pulling in shower energy based on a χ^2 shape criteria. A constraint on E/p matching would help terminate the process. Whatever is left is due to

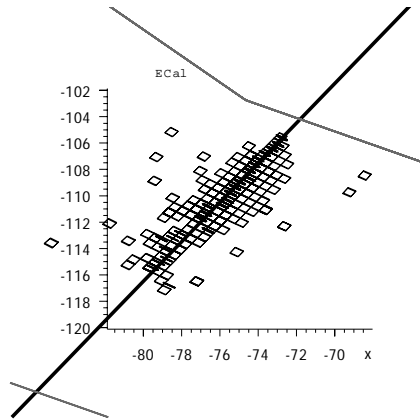


Figure 6. Photon “tracking” in the SD detector Si/W ECal. The small squares are hit cells. The shower profile is fit and extrapolated to the IP, shown as the dark line. The front face of the ECal is at the upper right. Based on a GEANT4 simulation. Figure from T. Abe.



Figure 7. Simulation of a 300 GeV τ with the decay mode $\tau \rightarrow \rho\nu \rightarrow \pi^+\pi^0\nu$ in the TESLA Si/W ECal and digital HCal. Figure from H. Videau.

neutral hadrons (subject to reasonable consistency constraints). And one gets reasonable muon identification as part of the process.

The “digital” HCal, discussed further below, pushes the transverse segmentation to ~ 1 cm. This approach is being pursued as an option for TESLA and with the SD detector. At this time, sharp criteria for HCal segmentation are still being developed. So it may be the case that a practical compensating technology like Pb and scintillating tiles can also provide adequate segmentation. This path is being pursued with the JLC and LD detectors.

We note that all designs to date have been able to put both ECal and HCal inside the solenoid coil, even with the large fields being pursued at the LC. Of course, this is beneficial to calorimeter resolution if it can be achieved. This is aided by the fact that the HCal at the LC does not have to be nearly as deep as those at a hadron collider, perhaps even more so for highly segmented

calorimeters which allow tracking of MIPs.

4.4. Limits to Jet Resolution

It is interesting to evaluate jet measurement using the energy flow technique in the case where the reconstruction algorithms are capable of correctly matching all energy depositions with the corresponding particle, *i.e.* perfect pattern recognition. Using the process $e^+e^- \rightarrow q\bar{q}$ as a benchmark, Figure 8 gives a sample jet-jet mass distribution. And Figure 9 gives the jet energy resolution as a function of E_{jet} . The width of the peak in the mass distribution is dominated by the ECal resolution for photons ($\approx 0.15/\sqrt{E}$), while the tails result from fluctuations of neutral hadrons and neutrinos.

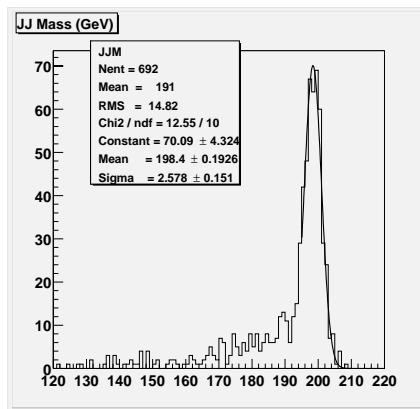


Figure 8. Jet-jet mass distribution for $e^+e^- \rightarrow q\bar{q}$ at 200 GeV in the SD detector in the limit of perfect pattern recognition.

The fit in Figure 9 gives a resolution of $0.15/\sqrt{E_{\text{jet}}}$. This agrees with the result derived² using a formulaic approach. The agreement demonstrates that fluctuations in particle types are unimportant, the resolution is limited by detector resolution, and QCD effects are relatively unimportant. This is in dramatic contrast to the case for hadron colliders, where detector resolution is in fact nearly negligible³ compared to QCD and underlying event effects.

The ideal result should also be compared with simulations from the TESLA group, which give jet energy resolution of $\sigma_E/E = 0.30/\sqrt{E_{\text{jet}}}$ for $e^+e^- \rightarrow q\bar{q}$ with realistic simulations, as shown at the previous meeting⁴ in this series. So presently there is a factor two between the ideal case and an existing reconstruction. Presumably, some of this difference can be reduced by the development and improvement of reconstruction algorithms.

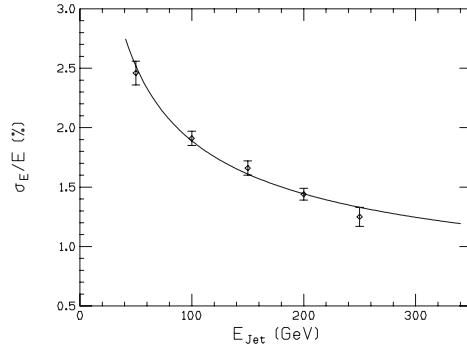


Figure 9. Jet energy resolution for $e^+e^- \rightarrow q\bar{q}$ as a function of E_{jet} in the SD detector in the limit of perfect pattern recognition.

To summarize, these studies allow one to make two general points: (1) LC jet resolution will be limited by detector resolution, not by QCD or other effects not under the control of the experimenter. (Nevertheless, it is still important to quantify QCD effects, which are likely to become more important for final states with many jets.) (2) The jet resolution will be in the range $(0.15 \text{ to } 0.30)/\sqrt{E_{\text{jet}}}$ (for 2-jet final states) for the TESLA or SD type of detector (see next section). It is important that proponents of various calorimeter designs be able to compare resolutions using equivalent full simulations, eventually reinforced by test beam results.

5. Design Ideas

Table 1 summarizes some of the major calorimeter parameters for current detector designs. It should be noted that in some cases these parameters are rapidly evolving, and are likely to soon be obsolete, if they are not already. The TESLA parameters are based on the TDR from 2001, except that the Shashlik ECal option is no longer included. In the discussion below, we note some recent changes and highlight some areas of R&D activity. The JLC parameters are based on the recent (July 2002) 3T design in the ACFA report.

5.1. TESLA

The calorimeter for TESLA consists of a highly-segmented (imaging), silicon-tungsten (Si/W) ECal. There are two options for the HCal, one using scintillating tile detectors and the other a “digital” HCal discussed below. Both HCal options use the same mechanical layout. The barrel ECal consists of eight modules, a few of which can be seen in the figure. In the design from

Table 1. Parameters of calorimeter designs currently under consideration. Note that many parameters will change as designs evolve. The labels T and D refer to two TESLA design options.

	TESLA ⁵	SD ⁶	LD ⁶	JLC ⁷
Tracker type	TPC	Silicon	TPC	Jet-cell drift
<u>ECal</u>				
R_{\min} barrel (m)	1.68	1.27	2.00	1.60
Type	Si pad/W	Si pad/W	scint. tile/Pb	scint. tile/Pb
Sampling	$30 \times 0.4X_0$ $+10 \times 1.2X_0$	$30 \times 0.71X_0$	$40 \times 0.71X_0$	$38 \times 0.71X_0$
Gaps (active) (mm)	2.5 (0.5 Si)	2.5 (0.3 Si)	1 (scint.)	1 (scint.)
Long. readouts	40	30	10	3
Trans. seg. (cm)	≈ 1	0.5	5.2	4
Channels ($\times 10^3$)	32000	50000	135	5
z_{\min} endcap (m)	2.8	1.7	3.0	1.9
<u>HCal</u>				
R_{\min} (m) barrel	1.91	1.43	2.50	2.0
Type	T: scint. tile/S.Steel D: digital/S.Steel	digital	scint. tile/Pb	scint. tile/Pb
Sampling	$38 \times 0.12\lambda$ (B), $53 \times 0.12\lambda$ (EC)	$34 \times 0.12\lambda$	$120 \times 0.047\lambda$	$130 \times 0.047\lambda$
Gaps (active) (mm)	T: 6.5 (5 scint.) D: 6.5 (TBD)	1 (TBD)	2 (scint.)	2 (scint.)
Longitudinal readouts	T: 9(B), 12(EC) D: 38(B), 53(EC)	34	3	4
Transverse segmentation (cm)	T: 5–25 D: 1	1	19	14
θ_{\min} endcap	5°	2°	2°	8°
<u>Coil</u>				
R_{\min} (m)	3.0	2.5	3.7	3.7
B (T)	4	5	3	3
Comment	Shashlik ECal option in TDR discontinued		option: Si pad shower max. det.	scint. strip (1 cm) shower max. det. (2 layers)

the TDR,⁵ the ECal front end electronics is at the edges of each module, positioned to be out sight of the IP. The readout end of the detector slab is shown in Figure 11. Recently, an alternative design has been developed which inserts the front end electronics within the slab. This has several advantages,⁸ but requires more attention to thermal management. Cost is always a concern for silicon detectors. In the TESLA TDR, the silicon detectors are about 70% of

the ECal cost While the TDR design included 40 Si layers, an alternative design with coarser sampling (20 layers) would reduce expense with a corresponding increase in photon resolution (0.11 to $0.14/\sqrt{E}$). A conservative estimate of the cost in 2005-10 for these relatively simple silicon detectors is $\$2/\text{cm}^2$. This puts the ECal cost estimate at roughly 70 MEuros for the 20-layer design.

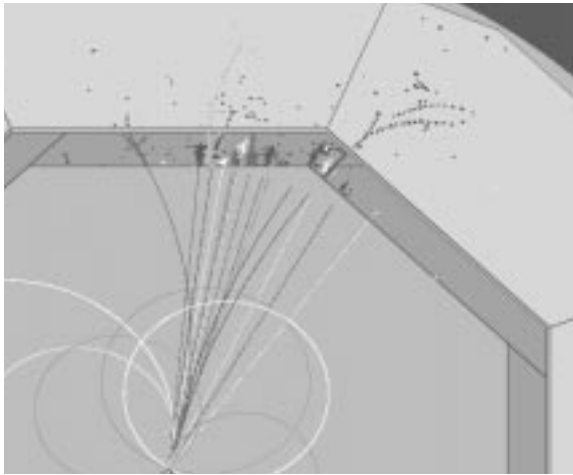


Figure 10. Simulated event in the TESLA detector with the digital HCal option.

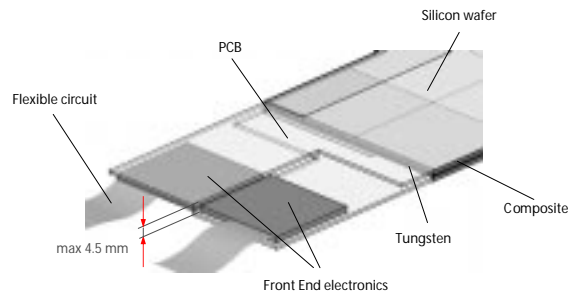


Figure 11. The end of the Si/W detector slab from the TESLA TDR design.

The tile HCal option was discussed in detail by Korbel⁹ at this meeting. The digital HCal option calls for enough segmentation so that a one bit readout suffices. This offers the possibility of a greatly simplified readout which can offset the cost of the increased segmentation. The current design calls for 1 cm

transverse segmentation. Figure 12 compares single particle resolution for the usual analog sum of HCal cells to the “digital” sum, that is, the multiplicity of hit cells. We see that the digital resolution is actually slightly better than that for the analog sum. An R&D effort is underway to choose an appropriate detector for this option. RPC detectors, if made to operate reliably, might be a good choice. A glass RPC, being considered for TESLA, is shown in Figure 13.

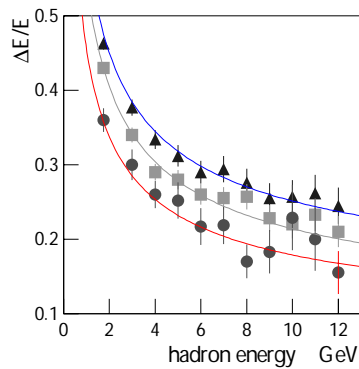


Figure 12. Comparison of single hadron energy resolution for a sum of the full energy of hit cells (triangles) and the digital sum (squares). The circles are after additional pattern recognition is applied to the digital hits. Figure from H. Videau.

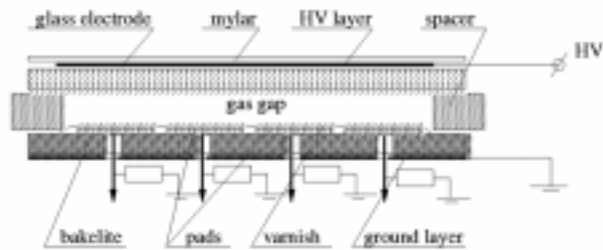


Figure 13. A glass RPC being considered for the TESLA digital HCal option. Figure from V. Amassov.

5.2. JLC Detector

The ACFA/JLC detector is based on a hardware compensating configuration of Pb and scintillating tile layers in the ratio 4:1. This structure has already

undergone extensive test beam evaluation, an example of which is given in Figure 14. One challenge for this design is whether the segmentation, both transverse and longitudinal, is sufficient, especially for the ECal. To aid spatial separation, a shower maximum detector is foreseen, consisting of one x and one y layer of scintillating strips. Another challenge is the readout of the light from the scintillator, which is only 1 mm thick in the ECal. Hence, the photon detectors must have high gain, but be formatted to read out thousands of channels. Hence, the R&D for these devices is critical. Figure 15 shows a CCD-based device under investigation.

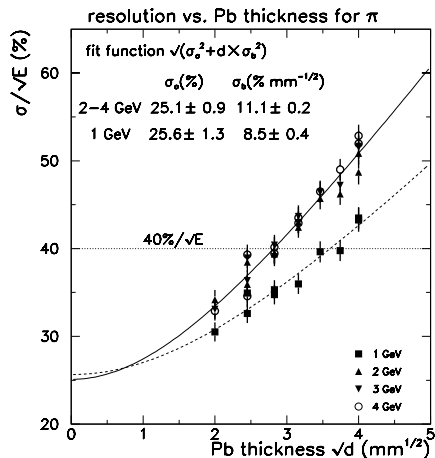


Figure 14. Test beam energy resolution for pions for the JLC Pb/scintillator configuration.

5.3. SD and LD

The SD detector being considered in N. America is a larger version of a detector first proposed at Snowmass 1996.¹⁰ The calorimeter for the current SD detector is similar to the TESLA design. It has a Si/W ECal and a digital HCal. The ECal R&D is currently focussed¹¹ on the issue of how to integrate detectors and electronics. A single readout chip mounted on a silicon wafer of pads would effectively reduce the readout channel count by a factor $\sim 10^3$. This is sketched in Figure 16. A simple cooling scheme may be possible if one uses power cycling to reduce the heat load by a factor $\sim 10^3$.

The SD digital HCal effort is investigating three different detector options:

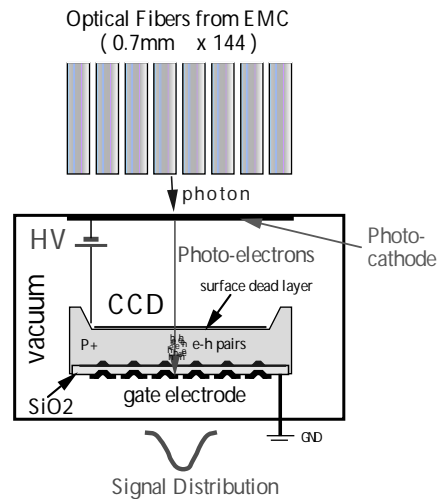


Figure 15. Pixelated photon detector being developed to readout the fibers from the JLC calorimeter scintillators. Figure from Y. Fujii.

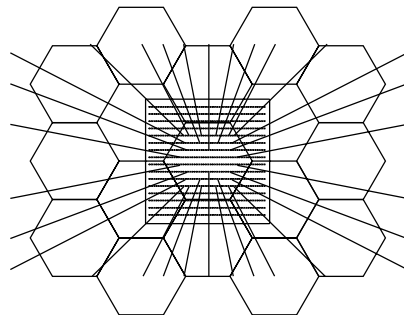


Figure 16. Center of a silicon detector wafer with 1000-channel readout chip bump bonded to the detector array. The detector pixels are hexagonal cells 5 mm across. A few representative signal traces are indicated.

RPCs, GEMs, and extruded scintillator tiles. The goal for each is to provide 1 cm segmentation at reasonable cost. The simple electronics possible with these technologies makes them compatible with the digital scheme. A GEM schematic is shown in Figure 17.

The LD calorimeter closely resembles the JLC detector. It exists as a configuration file for simulation studies, but currently no attempt has been made to provide a realistic design.

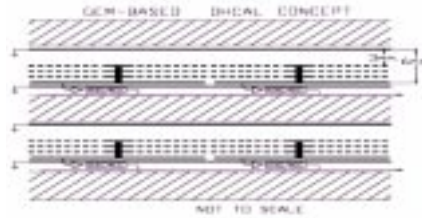


Figure 17. A schematic of a section of a gas electron multiplier (GEM) being considered for the SD digital HCal. Figure from A. White.

6. Prospects

Calorimeters are being designed to take full advantage of the wonderful detector environment at an LC. The most important criteria are based on detector-wide measurements, such as jet reconstruction. This is an interesting time in this development: There are new ideas to implement, test, and compare with alternatives. The energy flow methods are not simple to test, since to work well they require a full set of pattern recognition and reconstruction tools. Test beam measurements will be required to compare with full simulation results. R&D is required to answer both basic and detailed questions. We do not know now what the new physics will be at the LC, but hopefully the choices being made now will improve the discovery reach!

Acknowledgements

This work is supported in part by the US Department of Energy under award DE-FG02-96ER40969.

References

1. S. Kunori, these proceedings.
2. V. Morgunov, these proceedings.
3. D. Green, these proceedings.
4. H. Videau, Proc. Calor 2000, <http://www.lapp.in2p3.fr/Calor2000/>.
5. The TESLA TDR, http://tesla.desy.de/new_pages/TDR_CD/start.html, DESY, March 2001.
6. The American Linear Collider Working Group, "Resource Book for Snowmass 2001, Part IV," hep-ex/0106058, 2001.
7. ACFA LC Working Group Report, <http://acfahep.kek.jp/acfareport/>.
8. H. Videau, these proceedings.
9. V. Korbelt, these proceedings.
10. C. Damerell, et al., pg. 431, and J. Brau, et al., pg. 437, Proc. Snowmass 1996, www.slac.stanford.edu.
11. R. Frey, these proceedings.